WARSAW UNIVERSITY OF TECHNOLOGY Index 351733
FACULTY OF CIVIL ENGINEERING
COMMITTEE FOR CIVIL AND WATER ENGINEERING
POLISH ACADEMY OF SCIENCES ISSN 1230-2945

DOI: 10.24425/ace.2020.136467

ARCHIVES OF CIVIL ENGINEERING

Vol. LXVII ISSUE 1 2021

ANISOTROPY OF SOIL SHEAR STRENGTH PARAMETERS CAUSED BY THE PRINCIPAL STRESS ROTATION

G. WRZESIŃSKI[1]

The paper presents the phenomenon of principal stress rotation in cohesive subsoil resulting from its loading or unloading and the impact of this phenomenon on the values of soil shear strength parameters: undrained shear strength τ_{fu}, effective cohesion c', effective angle of internal friction φ'. For this purpose, tests in a triaxial apparatus and torsional shear hollow cylinder apparatus on selected undisturbed cohesive soils: sasiCl, saclSi, clSi, Cl, characterized by different index properties were carried out. Soil shear strength parameters were determined at angle of principal stress rotation α equal to 0° and 90° in tests in triaxial apparatus and α equal to 0°, 15°, 30°, 45°, 60°, 75°, 90° in tests in torsional shear hollow cylinder apparatus. The results of laboratory tests allow to assess the influence of the principal stress rotation on the shear strength parameters that should be used to determine the bearing capacity of the subsoil.

Keywords**:** soil, undrained shear strength, effective cohesion, effective angle of internal friction, principal stress rotation, torsional shear hollow cylinder test, triaxial test

[1] PhD., Eng., Warsaw University of Life Sciences, Institute of Civil Engineering, Nowoursynowska 159, 02-776 Warsaw, Poland, e-mail: grzegorz_wrzesinski@sggw.edu.pl

1. INTRODUCTION

The basic feature determining the load capacity of the subsoil are soil shear strength parameters which include: undrained shear strength, cohesion and an angle of internal friction. The values of these parameters are determined on the basis of laboratory or field tests, whose determination methods have significantly developed over the years, and as a result the available measurement tools meet the highest accuracy standards. Undrained shear strength, cohesion and angle of internal friction are characteristic features of cohesive soils and describes the extremal reaction of loaded soil in undrained conditions. The cohesion and angle of internal friction are characteristic of non-cohesive soils and describe the extremal reaction of the soil loaded in drained conditions. The strength parameters mentioned are strictly related to Mohr-Coulomb criterion of failure.

The value of soil strength parameters depends on soil type, consistency, stress state, history, and on factors such as loading type and loading mode [1]. Soil type and consistency are the natural feature of soil and depend on where the soil occurs. Stress state, history, loading type and loading mode are associated with subsoil loading. In natural condition principal stresses (σ_1, σ_2, σ_3) coincide with vertical and horizontal directions. The loading or unloading of subsoil changes the stress state of the soil, and thereby causes principal stress rotation in comparison with the soil's initial state obtained during the sedimentation process [2]. These rotations arise when principal stress increment directions do not coincide with the current principal stress directions. Thus, the directions of action of all three principal stresses deviate from their original directions with the values of angles designated as α, β and γ (Fig. 1). It is assumed that the angles of principal stress rotation α, β, γ are equal and that is why the literature most often uses the designation of the angle of principal stress rotation as α. The phenomenon of principal stress rotation is observed in the construction of almost all types of geotechnical structures [3]. Studies carried out so far show a significant impact of the principal stress rotation on the soil shear strength parameters, e.g. [4-11]. The presented research were performed on cohesive soils with a natural and reconstructed structure. The results of these research show that the highest value of the strength parameters in most cases is obtained at the angle $\alpha = 0°$, while the principal stress rotation stress reduces this value by several to several dozen percent. However, the influence of the principal stress rotation on the soil shear strength parameters in laboratory tests is often overlooked because of the difficulty to achieve this phenomenon in laboratory conditions.

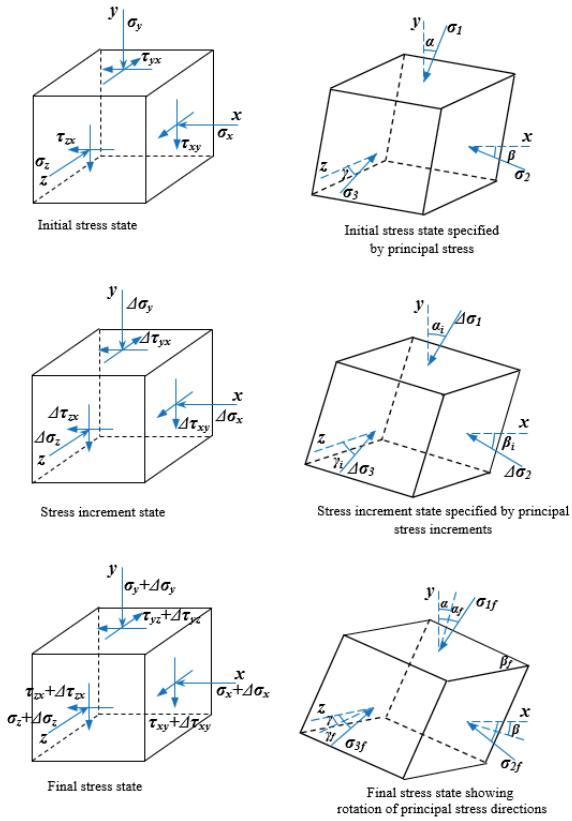

Fig. 1. Principal stress rotation in the soil element [2]

One of the ways to determine principal stress rotation due to changes in the load of subsoil is numerical analysis based on finite element method [3,12]. An example of numerical analysis of the stress state is the principal stress rotation analysis in the subsoil loaded with embankment performed by Jardine and Menkiti [13]. This analysis presents the lines with the same angle α of the values of principal stress rotation in the subsoil, resulting from the construction of the embankment on the soft-plastic clay (Fig. 2). As results from the calculations carried out, changes in the state of stress in the subsoil caused by the embankment with a height of 3 m do not only occur directly below the ground surface, but reach up to a depth of even above 10 m. On the basis of the lines with the same angle α, zones along the potential slip surface with the same soil damage mechanism can be determined.

The phenomenon of principal stress rotation in the subsoil, after loading or unloading the subsoil, causes various soil shear patterns which contribute to the anisotropy of shear strength parameters. In

literature, this phenomenon is most often called *forced anisotropy* [14,15]. Of course, the soil in natural conditions is usually an anisotropic material in terms of mechanical and physical properties which results, among others, from the arrangement of soil particles and the nature of contact between them and the distribution of pores. This phenomenon is called *structural anisotropy*. It is hard to separate the effects of both types of anisotropy, hence the subject of consideration is most often so-called *anisotropy* [16]. However, if the soil in the subsoil is homogeneous in terms of physical properties, the principal stress rotation is the basic factor causing anisotropy of shear strength parameters. In this case, determining the change in shear strength parameters in an appropriate test does not cause any difficulties.

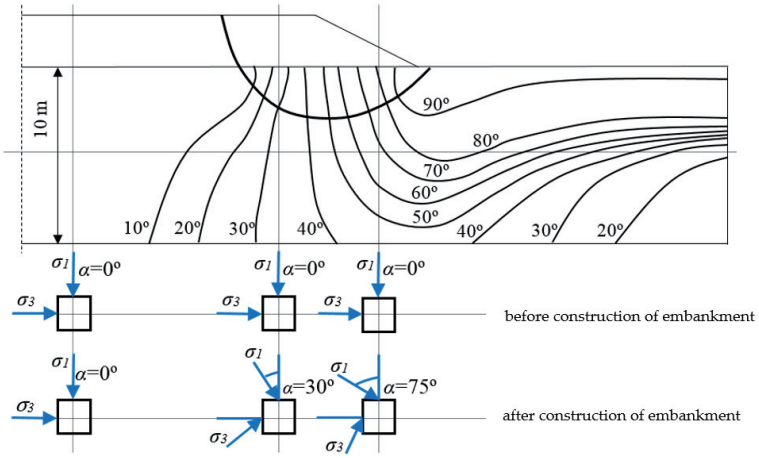

Fig. 2. Principal stress rotation in the subsoil loaded with embankment [13]

The impact of the principal stress rotation on the soil shear strength parameters in field tests is not a problem, since field tests measure the actual value of a parameter at a given depth in natural conditions. It should be noted that penetration of the test device changes the stress conditions themselves. Therefore, it is important to choose the right type of test for the type of research, and take this factor into account when analysing the test results. The problem is the restoration of natural conditions related to the principal stress rotation in laboratory tests. Attempts to determine soil shear strength parameters at different principal stress rotation in laboratory tests started in the mid-20th century. In the first research, attempts were made to investigate the impact of this phenomenon on the values of shear strength parameters using a direct shear apparatus [17], however, the uncontrolled rotation of principal stresses in the direct shear apparatus negatively affected the homogeneity of the

stress state and strain of the tested sample, which was demonstrated by Wright et al. [18]. Other attempts were undertaken to study the effect of this phenomenon in a three-axis apparatus by cutting samples at an angle α to the vertical direction [19-21], but this proved complicated in practice. Only the idea of using soil samples in the shape of a hollow cylinder allowed to start research works determining the impact of the principal stress directions on shear strength parameters under properly controlled boundary conditions. The first tests in a torsional shear hollow cylinder apparatus were carried out in the 1960s by Broms and Casbarian [22]. The test was carried out on hollow, cylindrical clay samples to determine the effect of the intermediate principal stress parameter and principal stress rotation on shear strength parameters. The tests showed that an increase in the value of the angle of rotation α causes an increase in water pressure in the pores with a simultaneous decrease in the value of shear strength parameters. Subsequently, this type of research was extended to determine the stress-strain characteristics for other soil types in drained and undrained conditions as well as for cyclic loads [23-26], by the use of piezoelectric transducers to measure transverse wave velocity [27].

The essence of laboratory tests enabling the determination of soil shear strength parameters is to obtain real values occurring in the subsoil. For this purpose, in addition to good quality and representative soil sample, of great importance is the testing equipment enabling the sample to be sheared according to the shear pattern observed in the field. Over the years, devices used to determine soil shear strength parameters have changed, undergone modifications, or new ones have been created to control additional factors [28]. Currently, there are many measuring tools that allow for more accurate measurements and a better way to save data. Of course, each device has a number of individual advantages and disadvantages, but the biggest advantage of laboratory tests is the ability to control the boundary conditions due to stress and deformation. Restrictions are mainly due to problems related to soil sampling with a fully intact structure, small sample volume limiting the representativeness of the entire soil profile and the lack of uniformity of stress and deformation during shearing [29].

Nowadays, to determine shear strength parameters at different principal stress rotation α in laboratory tests triaxial apparatus (TX) and torsional shear hollow cylinder apparatus (TSHCA) are used. Triaxial apparatus allows to determine soil shear strength parameters at the angle of principal stress rotation α only equal to 0° and 90°, while torsional shear hollow cylinder apparatus allows to determine shear strength parameters at any angle α. Triaxial apparatus [28], thanks to the appropriate construction and hydraulic method of setting the load, allows to control stress and boundary conditions, which in turn enables correct modeling of load changes in natural conditions. These features give the triaxial apparatus an advantage over other the laboratory equipment for soil shear strength testing. The device tests cylindrical samples surrounded by a rubber membrane and placed

in a pressure chamber filled most often with water. The soil sample is subjected to axially-symmetrical stress, and thus the intermediate principal stress σ_2 is equal to the lowest principal stress σ_3. Torsional shear hollow cylinder apparatus [2] allows to determine soil shear strength parameters at any angle of the principal stress rotation α. In this device hollow, cylindrical samples are tested. They are subjected to axial load P, torque M_T, inner and outer pressures, p_i and p_o. The torque M_T develops shear stresses $\tau_{\theta z}$ and $\tau_{z\theta}$ in vertical and horizontal planes, the axial load P contributes to a vertical stress σ_z, differences between p_o and p_i establish a gradient of radial stress σ_r across the cylindrical wall. Then, the circumferential stress σ_θ depends on radial stress σ_r and sample radius r and is determined according to the equation:

$$\sigma_\theta = \sigma_r + r\frac{d\sigma_r}{dr}$$

The hollow, cylindrical soil sample with particular stresses is presented in figure 3.

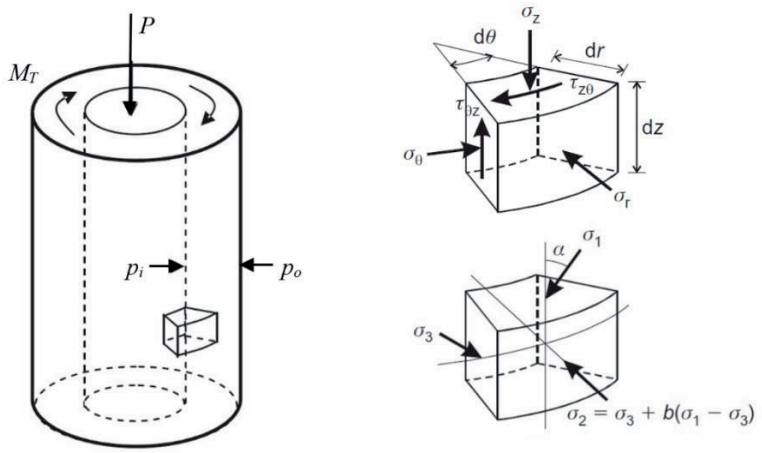

Fig. 3. Stresses acting on a hollow, cylindrical soil sample [2]

The major principal stress σ_1, intermediate principal stress σ_2 and minor principal stress σ_3 are defined as follows [2]:

$$\sigma_1 = \frac{\sigma_z + \sigma_\theta}{2} + \sqrt{\left(\frac{\sigma_z - \sigma_\theta}{2}\right)^2 + \tau_{\theta z}^2}$$

$$\sigma_2 = \sigma_r$$

$$\sigma_3 = \frac{\sigma_z + \sigma_\theta}{2} - \sqrt{\left(\frac{\sigma_z - \sigma_\theta}{2}\right)^2 + \tau_{\theta z}^2}$$

Values of angle of the principal stress rotation α and parameter of intermediate principal stress directions b are determined from the following equations [2]:

$$\alpha = \frac{1}{2} tg^{-1}\left(\frac{2\tau_{\theta z}}{\sigma_z - \sigma_\theta}\right)$$

$$b = \frac{\sigma_2 - \sigma_3}{\sigma_1 - \sigma_3}$$

Testing the hollow, cylindrical soil sample causes stress non-uniformity in the sample. To reduce the impact of stress non-uniformity on test results the length of soil sample l and the ratio of the inner radius r_i to the outer radius r_o should be as follows [28]:

$$l \geq 5{,}44\sqrt{r_o^2 - r_i^2}$$

$$\frac{r_i}{r_o} \geq 0.65$$

The analyzes showed that in case of the ratio of the inner radius r_i to the outer radius r_o equal to 0.65, the maximum level of stress non-uniformity occurring in the sample is 16% which is an acceptable value. Research shows that with the higher value of this ratio, the more stress non-uniformity occurs at a lower level [28].

The paper presents test results performed in a triaxial apparatus and torsional shear hollow cylinder apparatus on cohesive and non-cohesive soils characterized by different index properties. The main objective of the tests was to determine the soil shear strength parameters at wide range of angles of the principal stress rotation α. The results of laboratory tests allow to assess the influence of the principal stress rotation on the value of soil shear strength parameters that should be used to determine the bearing capacity of the subsoil.

2. MATERIALS AND METHODS

The laboratory tests to determine soil shear strength parameters were performed using the triaxial apparatus and torsional shear hollow cylinder apparatus. The research was carried out on overconsolidated cohesive soils characterized by a overconsolidation ratio *OCR* in the range from from 1.1 to 5.7 and plasticity index I_p in the range from 10% to 83.8%. The index properties of the tested soils are presented in table 1.

Tests in a triaxial apparatus (Fig. 4) were performed on cylindrical soil samples with a height of 100 mm and a diameter of 50 mm. A soil sample in the shape of a cylinder prepared for testing is presented in figure 5. In triaxial apparatus tests with isotropic consolidation and shearing in undrained conditions (TXCIU) were performed. Based on these tests the undrained shear strength τ_{fu}, angle of internal friction φ' and cohesion c' were determined.

The triaxial tests were performed in the following stages: flushing, saturation, anisotropic consolidation and shearing. The flushing was carried out to remove air and gases that have the largest dimensions from the samples and tubes. The saturation of the soil samples was performed using the back pressure method [29]. This stage lasted until the value of the Skempton's parameter B exceeded 0.90. Consolidation was performed to dissipate the excess of pore water pressure. After the dissipation of the excess of pore water pressure samples shearing in undrained conditions were performed. The shear of the soil sample at the angle $\alpha = 0°$ was carried out by increasing the vertical stress σ_1 while maintaining a constant horizontal stress σ_3. The shear of the sample at the angle $\alpha = 90°$ was carried out by increasing the horizontal stress σ_3 while maintaining the constant vertical stress σ_1.

The tests were carried out at various effective mean stress p' at the end of the consolidation stage. These values were in the range from 80 to 370 kPa. To determine shear strength parameters maximum deviator stress was used as a failure criterion. All the obtained values of undrained shear strength were normalized based on the in situ vertical effective stress component σ'_v to obtain comparable values of the normalized undrained shear strength independent on the value of the in situ effective stress.

Tests in a torsional shear hollow cylinder apparatus (Figure 6) were performed on hollow, cylindrical soil samples with a height of 200 mm, outside diameter of 100 mm and inside diameter of 60 mm. The hollow, cylindrical soil sample prepared for testing in the torsional shear hollow cylinder apparatus, is presented in figure 7. Samples in the shape of a hollow cylinder were prepared using a specialized machine tool consisting of a metal casings, a cutting knife and foil to prevent mechanical damage to the sample. During the preparation of the samples, special care was taken not to disturb the natural structure of the samples. This was particularly important as samples were prepared with a wide range of consistency parameters ($I_L = –0.16 \div 0.86$). The shear strength parameters for particular soil type were determined at following angles of the principal stress rotation α: 0°, 15°, 30°, 45°, 60°, 75°, 90°.

Table 1. Index properties of tested cohesive soils

No.	Soil [30]	Fraction [31] (%)				*OCR* (-)	w_n (%)	w_L (%)	w_P (%)	I_P (%)	I_L (-)	I_C (-)
		Gr	*Sa*	*Si*	*Cl*							
1	sasiCl	0	25	47	28	2.4	31.9	52.3	21.8	30.5	0.33	0.67
2	sasiCl	0	21	50	29	2.7	28.8	59.0	24.3	34.7	0.13	0.87
3	sasiCl	0	28	48	24	3.2	31.1	49.5	23.9	25.6	0.28	0.72
4	sasiCl	0	34	46	20	3.5	28.5	42.6	22.5	20.1	0.30	0.70
5	sasiCl	0	23	51	26	4.0	27.1	43.9	17.3	26.6	0.37	0.63
6	sasiCl	0	30	43	27	4.4	25.3	50.1	22.9	27.2	0.09	0.91
7	sasiCl	1	50	37	12	2.0	14.0	24.2	12.2	12.0	0.15	0.85
8	sasiCl	0	16	66	18	1.8	26.6	34.2	19.9	14.3	0.47	0.53
9	sasiCl	2	50	46	2	1.4	19.3	20.7	10.7	10.0	0.86	0.14
10	sasiCl	0	58	30	12	2.3	10.0	25.0	12.1	12.9	-0.16	1.16
11	sasiCl	0	47	36	17	3.2	14.6	23.3	12.6	10.7	0.19	0.81
12	sasiCl	2	48	37	13	1.1	9.9	22.4	11.5	10.9	-0.15	1.15
13	sasiCl	1	41	43	15	1.8	21.0	28.3	10.9	17.4	0.58	0.42
14	sasiCl	1	27	55	17	1.5	15.9	24.5	11.7	12.8	0.33	0.67
15	saclSi	0	10	74	16	2.5	36.3	61.0	33.1	27.9	0.12	0.88
16	saclSi	0	24	67	9	2.3	20.2	28.6	16.5	12.1	0.69	0.31
17	saclSi	0	17	69	14	1.9	21.8	32.7	14.9	17.8	0.39	0.61
18	saclSi	0	18	68	14	1.6	29.6	40.9	21.3	19.6	0.42	0.58
19	saclSi	0	21	64	15	1.7	25.8	39.2	15.2	24.0	0.44	0.56
20	saclSi	0	20	66	14	1.1	20.3	36.4	14.8	21.6	0.25	0.75
21	clSi	0	12	70	18	2.4	18.5	51.9	19.5	32.4	-0.03	1.03
22	clSi	0	18	52	30	2.1	20.5	74.5	23.7	50.8	-0.06	1.06
23	clSi	0	17	59	24	2.0	20.3	65.8	22.1	43.7	-0.04	1.04
24	clSi	0	15	65	20	1.7	19.2	59.8	20.9	38.9	-0.04	1.04
25	clSi	0	10	62	28	1.8	18.4	70.6	24.5	46.1	-0.13	1.13
26	clSi	0	16	60	24	1.4	21.5	60.4	22.3	38.1	-0.02	1.02
27	clSi	0	15	62	23	1.1	17.8	58.7	18.2	40.5	-0.01	1.01
28	Cl	0	12	48	40	4.3	26.9	99.7	32.8	66.9	-0.09	1.09
29	Cl	0	8	36	56	4.0	27.8	108.9	32.7	76.2	-0.06	1.06
30	Cl	0	5	36	59	2.8	31.2	102.5	29.8	72.7	0.02	0.98
31	Cl	0	14	47	39	3.0	26.5	69.6	30.3	39.3	-0.10	1.10
32	Cl	0	4	31	65	4.2	28.3	114.8	36.1	78.7	-0.10	1.10
33	Cl	0	6	36	58	3.7	30.4	112.9	35.3	77.6	-0.06	1.06
34	Cl	0	3	42	55	4.2	32.5	110.0	31.2	78.8	0.02	0.98
35	Cl	0	4	48	48	5.7	26.9	120.3	36.5	83.8	-0.11	1.11

Notes:

OCR – overconsolidation ratio, w_n – water content, w_L – liquid limit, w_p – plastic limit, I_p – plasticity index, I_L – liquidity index, I_C – consistency index, *Gr* – gravel, *Sa* – sand, *Si* – silt, *Cl* – clay.

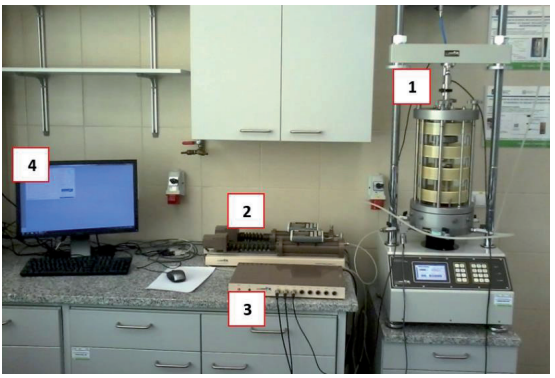

Fig. 4. Triaxial apparatus (TX) used in tests: 1 – cell, 2 – pressure and volume controllers, 3 – electronic measuring device, 4 – computer to control the test [34]

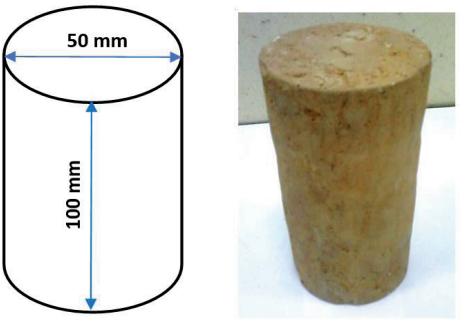

Fig. 5. A soil sample in the shape of a cylinder prepared for testing in a triaxial apparatus [34]

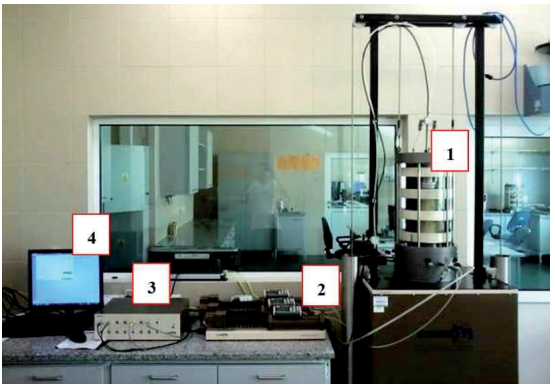

Fig. 6. Torsional shear hollow cylinder apparatus (TSHCA) used in tests; 1 – TSHC apparatus cell, 2 – pressure and volume controllers, 3 – electronic measuring device, 4 – computer to control test [34]

Fig. 7. Soil sample in the shape of hollow cylinder prepared for testing in a torsional shear hollow cylinder apparatus [34]

The torsional shear hollow cylinder tests were performed in the following stages: flushing, saturation, anisotropic consolidation, change of parameter of intermediate principal stress directions b, change of angle of the principal stress rotation α, shearing in undrained conditions. Flushing was carried out to remove air and gases having the largest dimensions from the samples and tubes. Saturation of soil samples was performed using the back pressure method. This stage lasted until the value of the Skempton's parameter B exceeded 0.90. After dissipation of excess pore water pressure, parameter b started to change to a value of 0.5. In the next step, the value of angle α changed to the determined value in a particular test. Finally, the process of sample shearing was carried out in the stress path involving the increase in the deviator stress q and constant value of the total mean stress p. During the entire shearing process of the soil samples, constant values of parameter b and angle α were kept.

3. RESULTS

The tests in triaxial apparatus and torsional shear hollow cylinder apparatus allowed to obtain the values of the shear strength parameters (undrained shear strength τ_{fu}, effective cohesion c' and effective angle of internal friction φ') at a selected angle of the principal stress rotation α for particular soils. Shear strength parameters for soils tested in triaxial apparatus are presented in table 2, while shear strength parameters for soils tested in torsional shear hollow cylinder apparatus are presented in tables 3-5. To determine these parameters the maximum deviator stress was used as the failure criterion. All the obtained values of the undrained shear strength τ_{fu} were normalized based on the in situ vertical effective stress component σ'_v to obtain comparable values of the normalized undrained

shear strength independent on the value of the in situ effective stress. Axial strains corresponding to the obtained values of the shear strength parameters were in the range of 7.1–16.5%.

Table 2. Shear strength parameters for tested soils in triaxial apparatus

No.	Soil	Angle of the principal stress rotation α (°)					
		0	90	0	90	0	90
		Normalized undrained shear strength τ_{fu}/σ'_v (-)		Effective cohesion c' (kPa)		Effective angle of internal friction φ' (°)	
1	sasiCl	0.601	0.522	25.7	18.6	18	12
2	sasiCl	0.514	0.431	23.6	15.4	19	15
3	sasiCl	0.580	0.498	18.3	13.4	20	17
4	sasiCl	0.703	0.487	20.5	16.5	19	12
5	sasiCl	0.498	0.375	24.3	18.7	16	10
6	sasiCl	0.731	0.571	18.7	15.4	14	6
7	sasiCl	0.418	0.324	18.5	10.3	15	12
8	sasiCl	0.592	0.588	23.4	21.8	20	18
9	sasiCl	0.599	0.571	20.1	17.0	19	15
10	sasiCl	0.832	0.713	20.4	10.5	16	9
11	sasiCl	0.608	0.298	17.6	10.6	22	11
12	sasiCl	0.772	0.744	26.0	23.7	21	19
13	sasiCl	0.425	0.301	21.5	20.4	18	17
14	sasiCl	0.738	0.710	16.7	16.9	17	11
15	saclSi	0.530	0.476	21.8	12.7	16	9
16	saclSi	0.612	0.422	24.9	14.4	14	10
17	saclSi	0.481	0.398	21.5	20.3	14	15
18	saclSi	0.368	0.345	20.6	18.1	15	14
19	saclSi	0.391	0.374	24.3	21.8	14	10
20	saclSi	0.420	0.399	25.5	19.8	16	11
21	clSi	0.599	0.712	26.7	19.6	12	7
22	clSi	0.502	0.512	28.4	18.5	11	4
23	clSi	0.498	0.402	25.3	18.2	12	5
24	clSi	0.605	0.578	26.0	25.7	10	6
25	clSi	0.631	0.519	24.9	23.1	9	7
26	clSi	0.640	0.520	24.0	22.9	8	8
27	clSi	0.523	0.498	22.8	20.4	7	5
28	Cl	0.703	0.556	28.5	21.8	7	6
29	Cl	0.881	0.576	32.0	28.5	6	3
30	Cl	0.974	0.803	30.5	25.4	6	3
31	Cl	1.193	0.798	28.9	23.2	8	5
32	Cl	0.851	0.365	33.0	26.6	4	4
33	Cl	1.018	0.581	31.8	21.0	5	3
34	Cl	0.980	0.754	31.7	24.4	6	5
35	Cl	1.245	1.018	35.0	30.2	5	3

Table 3. Normalized undrained shear strength τ_{fu}/σ'_v for tested soils in torsional shear hollow cylinder apparatus

No.	Soil	Angle of the principal stress rotation α (°)						
		0	15	30	45	60	75	90
		Normalized undrained shear strength τ_{fu}/σ'_v (-)						
1	sasiCl	0.640	0.626	0.596	0.593	0.576	0.571	0.564
2	sasiCl	0.588	0.572	0.535	0.485	0.461	0.454	0.447
3	sasiCl	0.615	0.580	0.570	0.524	0.517	0.506	0.504
4	sasiCl	0.734	0.716	0.697	0.656	0.630	0.616	0.590
5	sasiCl	0.530	0.528	0.507	0.482	0.475	0.460	0.458
6	sasiCl	0.750	0.741	0.706	0.654	0.628	0.621	0.603
7	sasiCl	0.450	0.443	0.428	0.410	0.392	0.385	0.381
8	sasiCl	0.629	0.621	0.607	0.581	0.598	0.600	0.627
9	sasiCl	0.693	0.668	0.645	0.574	0.603	0.651	0.680
10	sasiCl	0.894	0.892	0.883	0.851	0.822	0.761	0.783
11	sasiCl	0.631	0.580	0.521	0.490	0.389	0.360	0.363
12	sasiCl	0.783	0.770	0.739	0.674	0.692	0.743	0.760
13	sasiCl	0.432	0.418	0.400	0.320	0.382	0.388	0.403
14	sasiCl	0.740	0.693	0.590	0.523	0.610	0.690	0.723
15	saclSi	0.549	0.540	0.533	0.520	0.520	0.508	0.509
16	saclSi	0.632	0.630	0.618	0.599	0.527	0.501	0.480
17	saclSi	0.499	0.449	0.440	0.411	0.416	0.417	0.417
18	saclSi	0.471	0.468	0.413	0.390	0.393	0.399	0.400
19	saclSi	0.487	0.454	0.390	0.318	0.326	0.389	0.448
20	saclSi	0.450	0.441	0.403	0.401	0.423	0.438	0.447
21	clSi	0.780	0.780	0.778	0.773	0.764	0.745	0.743
22	clSi	0.676	0.671	0.670	0.634	0.628	0.579	0.577
23	clSi	0.632	0.618	0.611	0.565	0.543	0.517	0.490
24	clSi	0.703	0.689	0.676	0.649	0.640	0.693	0.698
25	clSi	0.742	0.670	0.585	0.512	0.602	0.675	0.736
26	clSi	0.721	0.708	0.685	0.620	0.673	0.694	0.708
27	clSi	0.632	0.620	0.587	0.590	0.604	0.621	0.630
28	Cl	0.898	0.887	0.865	0.832	0.762	0.711	0.657
29	Cl	0.950	0.950	0.919	0.881	0.834	0.769	0.700
30	Cl	1.034	1.008	1.001	0.997	0.983	0.947	0.923
31	Cl	1.286	1.254	1.206	1.198	1.106	1.054	0.912
32	Cl	0.984	0.912	0.845	0.743	0.611	0.536	0.489
33	Cl	1.176	1.165	1.023	0.910	0.876	0.804	0.670
34	Cl	0.996	0.990	0.942	0.895	0.878	0.843	0.835
35	Cl	1.336	1.294	1.183	1.178	1.098	1.079	1.067

Table 4. Effective cohesion *c*' for tested soils in torsional shear hollow cylinder apparatus

No.	Soil	Angle of the principal stress rotation α (°)						
		0	15	30	45	60	75	90
		Effective cohesion *c'* (kPa)						
1	sasiCl	26.1	23.2	23.0	22.5	21.8	21.2	19.8
2	sasiCl	25.0	23.7	22.6	20.5	18.9	18.3	17.5
3	sasiCl	18.9	17.3	16.5	16.1	15.3	14.2	13.6
4	sasiCl	21.4	21.1	20.2	19.5	18.4	17.9	17.2
5	sasiCl	24.7	24.0	22.5	21.6	20.9	20.7	19.8
6	sasiCl	21.0	19.5	19.4	18.1	17.5	16.8	16.9
7	sasiCl	19.8	18.3	16.5	15.4	13.2	13.0	11.5
8	sasiCl	24.5	22.1	21.9	19.8	20.2	21.1	23.4
9	sasiCl	21.6	19.4	18.7	16.5	17.1	17.4	18.9
10	sasiCl	20.3	19.5	18.9	16.8	14.2	13.6	13.1
11	sasiCl	18.6	17.0	15.9	14.7	13.7	13.0	12.2
12	sasiCl	26.4	24.9	23.1	20.2	20.8	23.6	24.0
13	sasiCl	21.7	20.1	17.3	15.5	17.9	19.3	21.9
14	sasiCl	19.8	16.4	15.2	13.3	14.5	18.6	19.4
15	saclSi	22.5	19.6	19.3	17.5	16.2	15.0	13.7
16	saclSi	24.7	22.8	21.0	18.4	16.9	15.4	16.3
17	saclSi	22.1	21.3	20.4	17.8	17.7	18.9	21.0
18	saclSi	21.4	19.8	16.3	15.4	17.9	19.5	20.9
19	saclSi	25.0	22.5	18.4	16.7	19.8	22.6	24.3
20	saclSi	27.2	27.0	25.3	20.8	21.2	21.7	21.6
21	clSi	28.3	27.9	25.4	23.6	23.9	22.1	21.7
22	clSi	30.0	28.6	27.6	25.1	22.6	21.3	19.3
23	clSi	27.5	24.4	24.7	22.0	20.5	19.6	18.8
24	clSi	26.2	25.4	22.2	21.4	23.2	26.1	26.4
25	clSi	26.1	24.7	21.0	18.8	20.7	23.5	24.8
26	clSi	26.5	26.4	25.2	24.8	23.3	23.9	23.1
27	clSi	23.3	22.5	21.6	21.5	21.2	21.0	21.0
28	Cl	29.9	28.6	28.1	26.5	23.9	22.8	22.7
29	Cl	32.2	32.1	31.5	30.7	30.5	30.5	29.6
30	Cl	31.8	30.5	30.3	30.2	29.6	27.3	27.0
31	Cl	30.6	30.2	30.0	28.6	27.5	26.8	24.3
32	Cl	33.5	32.6	30.8	30.0	28.7	28.1	27.4
33	Cl	32.7	30.5	29.4	27.4	26.1	24.3	23.8
34	Cl	33.2	32.1	30.3	28.7	25.2	25.0	24.9
35	Cl	35.4	33.1	32.7	32.3	31.6	31.1	30.2

The test results showed that in most cases higher values of strength parameters (normalized undrained shear strength τ_{fu}/σ'_v, effective cohesion *c*', effective angle of internal friction φ') were obtained from the hollow cylinder tests compared to the triaxial tests. The correlation between the normalized undrained shear strength τ_{fu}/σ'_v, effective cohesion *c'* and effective angle of internal friction φ' for two selected soils are presented in Figures 8-13. The test results show that the soils, depending on

Table 5. Effective angle of internal friction φ' for tested soils in torsional shear hollow cylinder apparatus

No.	Soil	Angle of the principal stress rotation α (°)						
		0	15	30	45	60	75	90
		Effective angle of internal friction φ' (°)						
1	sasiCl	18	18	17	17	15	15	16
2	sasiCl	20	19	18	16	15	14	14
3	sasiCl	23	21	20	20	20	19	17
4	sasiCl	19	18	17	17	16	15	15
5	sasiCl	17	17	16	15	15	13	11
6	sasiCl	16	14	14	12	11	9	7
7	sasiCl	19	18	16	13	12	12	12
8	sasiCl	22	21	20	16	18	19	21
9	sasiCl	19	18	16	14	14	15	18
10	sasiCl	19	18	17	14	13	12	12
11	sasiCl	22	23	19	18	17	16	14
12	sasiCl	21	19	16	15	17	19	20
13	sasiCl	19	18	16	15	17	18	19
14	sasiCl	17	15	12	11	11	13	13
15	saclSi	16	16	15	15	13	12	12
16	saclSi	16	15	14	14	13	12	11
17	saclSi	17	16	16	14	14	15	17
18	saclSi	18	16	13	12	14	15	17
19	saclSi	15	15	13	10	11	11	13
20	saclSi	18	17	14	9	10	12	13
21	clSi	12	12	11	10	11	10	10
22	clSi	11	9	8	7	6	6	6
23	clSi	13	12	10	8	7	7	6
24	clSi	12	11	8	6	7	8	8
25	clSi	12	9	6	5	7	7	10
26	clSi	10	8	7	5	6	6	8
27	clSi	10	9	7	3	5	6	6
28	Cl	10	10	8	6	6	7	6
29	Cl	8	7	7	7	6	6	5
30	Cl	7	5	5	4	3	3	3
31	Cl	10	9	9	7	7	6	5
32	Cl	6	6	5	5	4	4	5
33	Cl	9	8	7	6	6	4	3
34	Cl	9	7	7	6	4	5	5
35	Cl	6	6	5	5	4	4	4

the overconsoilidation ratio *OCR*, have a different changes in strength parameters. Therefore, the Figures 14-20 show diagrams of the change in normalized undrained shear strength τ_{fu}/σ'_v for particular soil types, distinguishing between normally consolidated and lightly overconsolidated soils ($OCR < 2$) and overconsolidated soils ($OCR \geq 2$).

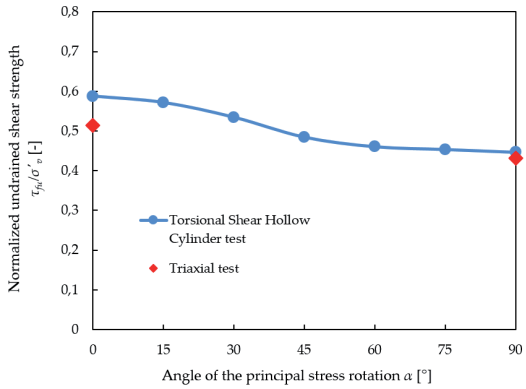

Fig. 8. Normalized undrained shear strength τ_{fu}/σ'_v for soil no. 2 - sasiCl

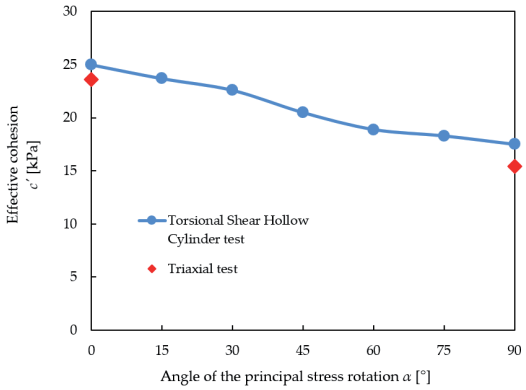

Fig. 9. Effective cohesion c' for soil no. 2 - sasiCl

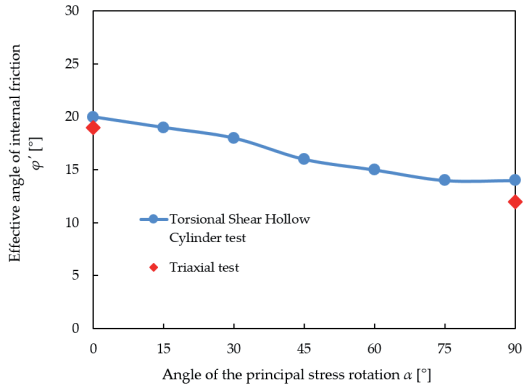

Fig. 10. Effective angle of internal friction φ' for soil no. 2 - sasiCl

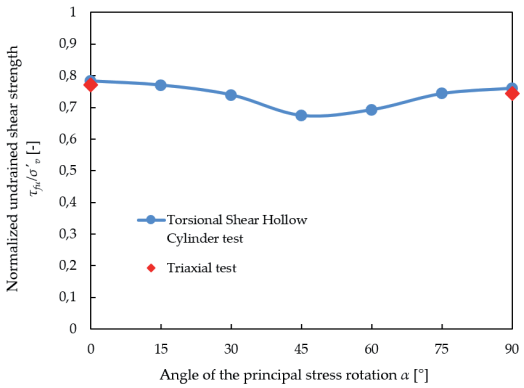

Fig. 11. Normalized undrained shear strength τ_{fu}/σ'_v for soil no. 12 - sasiCl

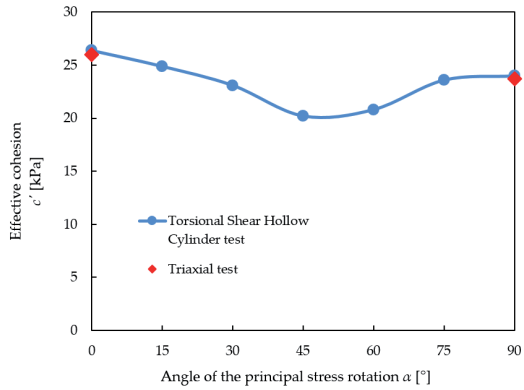

Fig. 12. Effective cohesion c' for soil no. 12 - sasiCl

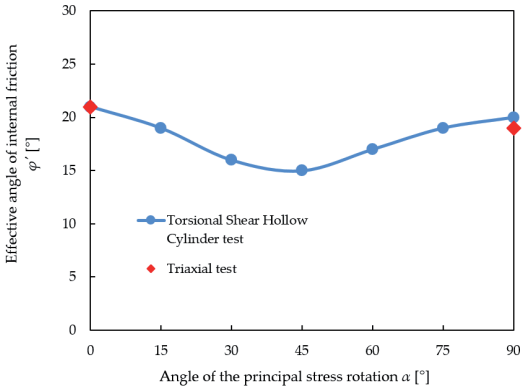

Fig. 13. Effective angle of internal friction φ' for soil no. 12 – sasiCl

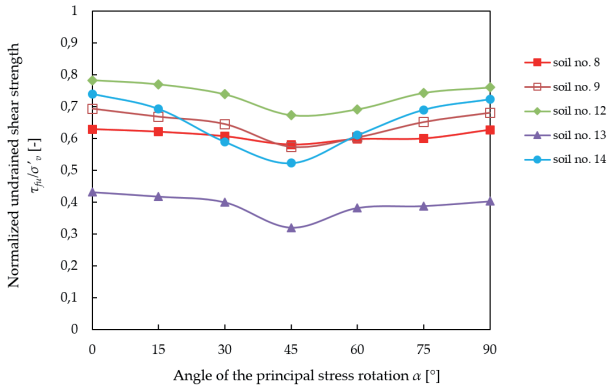

Fig. 14. Normalized undrained shear strength τ_{fu}/σ'_v for sasiCl with $OCR < 2$

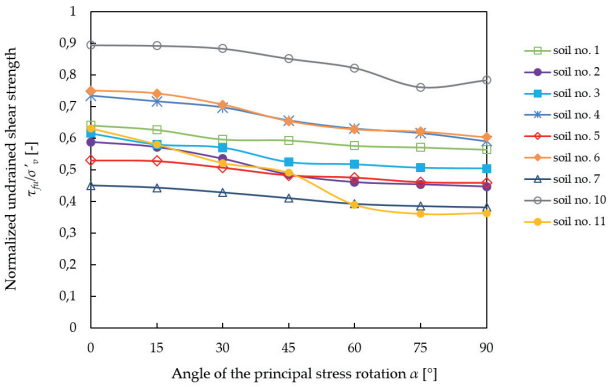

Fig. 15. Normalized undrained shear strength τ_{fu}/σ'_v for sasiCl with $OCR \geq 2$

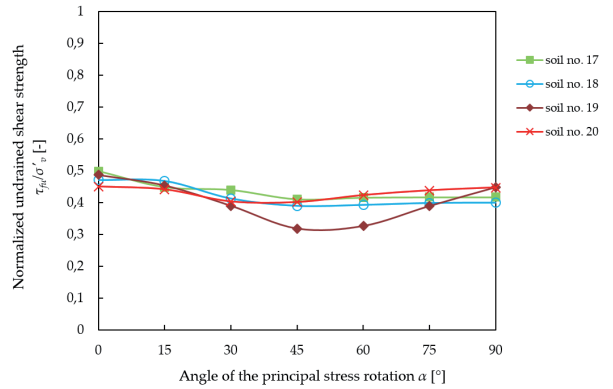

Fig. 16. Normalized undrained shear strength τ_{fu}/σ'_v for saclSi with $OCR < 2$

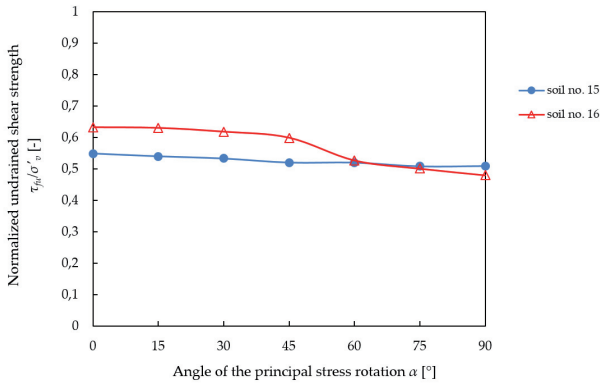

Fig. 17. Normalized undrained shear strength τ_{fu}/σ'_v for saclSi with $OCR \geq 2$

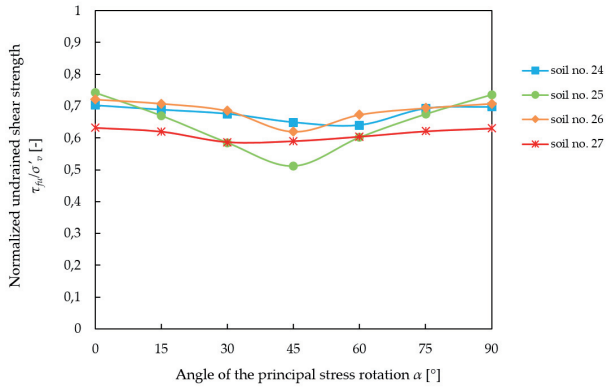

Fig. 18. Normalized undrained shear strength τ_{fu}/σ'_v for clSi with $OCR < 2$

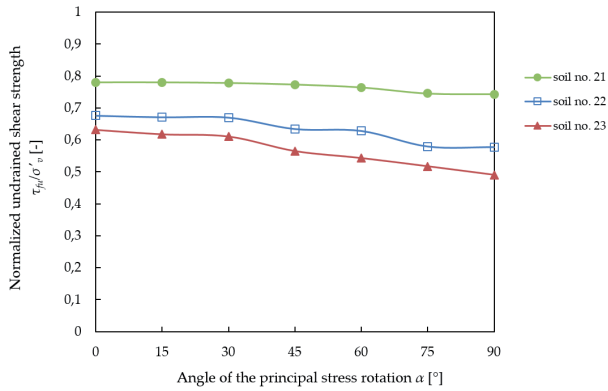

Fig. 19. Normalized undrained shear strength τ_{fu}/σ'_v for clSi with $OCR \geq 2$

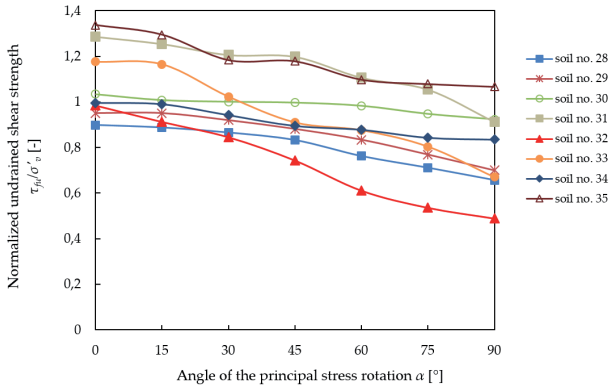

Fig. 20. Normalized undrained shear strength τ_{fu}/σ'_v for Cl with $OCR \geq 2$

4. DISCUSSION

The results of the research show that principal stress rotation in cohesive subsoil significantly affects the value of soil shear strength parameters: undrained shear strength τ_{fu}, effective cohesion c', effective angle of internal friction φ'. The tests performed both in the triaxial apparatus and torsional shear hollow cylinder apparatus showed that principal stress rotation causes the anisotropy of shear strength parameters in the subsoil. In normally consolidated soils and lightly overconsolidated soils ($OCR < 2$) the value of shear strength parameters is generally the lowest at an angle of principal stress rotation $\alpha = 45°$. In case of overconsolidated soils ($OCR \geq 2$) the value of shear strength parameters decreases with the increase of angle of the principal stress rotation α. However, the course of the decrease is different in particular soils. The analysis of the test results shows that in case of sandy silty clay (sasiCl) a higher decrease in the shear strength parameters occurs for angles α between 0° and 45°, whereas the decrease in the shear strength parameters is much smaller for angles above 45° for overconsolidated soils ($OCR \geq 2$). In some cases, the differences in the shear strength parameters are even around 40%. In general, it can be stated that for the same soil there is a similar trend of changing the measured shear strength parameters: undrained shear strength τ_{fu}, effective cohesion c', effective angle of internal friction φ' depending on the angle of principal stress rotation α.

Values of shear strength parameters obtained from triaxial tests and torsional shear hollow cylinder tests for the same angle of principal stress rotation α are comparable, however, for each soil slightly lower values of shear strength parameters in the triaxial apparatus were obtained. The differences

result from the control of other parameters in triaxial apparatus and torsional shear hollow cylinder apparatus.

The phenomenon of the principal stress rotation in the subsoil as a result of its loading or unloading is inevitable, and most of the existing methods of assessing the bearing capacity of the subsoil do not take into account its impact on the shear strength parameters. The probable reason is that for a long time there was a problem of including the principal stress rotation in laboratory tests. Only the possibility of testing hollow, cylindrical samples in a torsional shear hollow cylinder apparatus allowed to precisely measure the effect of principal stress rotation on soil shear strength parameters in laboratory tests. However, due to the costs of the apparatus and testing, it is not commonly used in test to determine the bearing capacity of subsoil. Shear strength parameters are commonly adopted for the entire subsoil as a representative value obtained in a triaxial apparatus in the test at the angle $\alpha = 0°$, which in case of tested soils leads to overestimation of the bearing capacity of the subsoil.

To determine the change of soil shear strength parameters depending on the principal stress rotation α, there are many empirical equations [32-36]. However, the use of these equations requires the prior determination of many physical properties of the investigated soil and is therefore rarely used.

In view of the above, bearing in mind changes in the state of stress in the subsoil as a result of loading or unloading it, and citing after Tavenas [37] that "*principal stress rotation in the subsoil is a rule, not an exception*", the Author concludes that the issue of change in shear strength parameters should not be overlooked when modeling the behaviour of the subsoil under load, and existing methods of assessing the bearing capacity of the subsoil require modification.

5. CONCLUSIONS

The tests performed in the triaxial apparatus and torsional shear hollow cylinder apparatus show that principal stress rotation causes the anisotropy of shear strength parameters (undrained shear strength τ_{fu}, effective cohesion c', effective angle of internal friction φ') in the cohesive subsoil. In normally consolidated soils ($OCR \approx 1$) the value of shear strength parameters is generally the lowest at an angle of principal stress rotation $\alpha = 45°$. In case of overconsolidated soils ($OCR \geq 2$) the value of shear strength parameters decreases with the increase of an angle of the principal stress rotation α.

The tests carried out in a triaxial apparatus at angles of $\alpha = 0°$ and $90°$ and in the torsional shear hollow cylinder apparatus at the same values of angles α show that for all cohesive soils a lower value of strength parameters was obtained in tests in a triaxial apparatus.

The phenomenon of principal stress rotation in the subsoil as a result of load changes is a common phenomenon, however, due to the difficulty in determining its impact on shear strength parameters in laboratory tests it is commonly ignored. This leads to the fact that in the calculation of the bearing capacity of the subsoil, only one value of the shear strength parameters determined at the angle $\alpha = 0°$ is most often used. Taking the value of the shear strength parameters determined at one angle of the principal stress rotation α for the entire subsoil most often leads to underestimation or overestimation of the actual value of the bearing capacity of the subsoil.

In order to determine the influence of the principal stress rotation α on shear strength parameters further research on soils, characterized by different index properties and modification of existing methods for determining the bearing capacity of the subsoil, should be carried out.

REFERENCES

1. R.J. Jardine, "One perspective of the pre-failure deformation characteristics of some geomaterials", Pre-failure Deformation of Geomaterials, Proc. Sapporo. Balkema Rotterdam, 2, pp 855-885, 1995.
2. D.W. Hight, A. Gens, M.J. Symes, "The development of a new hollow cylinder apparatus for investigating the effects of principal stress rotation in soils", Géotechnique 33, pp 335-383, 1983.
3. H.P. Neher, M. Cudny, C. Wiltafsky, H.F. Schweiger, "Modelling principal stress rotation effects with multilaminate type constitutive models for clay", Proc. of 8th International Symposium on Numerical Models in Geomechanics, Rome, pp 41-47, 2002.
4. W.H. Ward, S.G. Samuels, M.E. Butler, "Further studies of the properties of the London Clay", Géotechnique 9, pp 33-58, 1959.
5. J.H. Atkinson, "Anisotropic elastic deformations in laboratory tests on undisturbed London Clay", Géotechnique, pp 357-374, 1975.
6. R.J. Jardine, C.O. Menkiti, "The undrained anisotropy of K_o consolidated sediments". Proc. of 12th European Conference on Soil Mechanics and Geotechnical Engineering, Amsterdam, 2, pp 1101-1108, 1999.
7. P.V. Lade, M.M. Kirkgard, "Effects of stress rotation and changes of *b*-values on cross-anisotropic behavior of natural K_o consolidated soft clay", Soils and Foundations 40, pp 93-105, 2000.
8. H. Lin, D. Penumadu, "Experimental investigation on principal stress rotation in Kaolin Clay", Journal of Geotechnical and Geoenvironmental Engineering 131, pp 633-642, 2005.
9. S. Nishimura, N.A. Minh, R.J. Jardine, "Shear strength anisotropy of natural London Clay", Géotechnique 57, pp 49-62, 2007.
10. T. Shogaki, N. Kumagai, "A slope stability analysis considering undrained strength anisotropy of natural clay deposits", Soils and Foundations 48, pp 805-819, 2008.
11. G. Wrzesiński, Z. Lechowicz, "Influence of the rotation of principal stress directions on undrained shear strength", Annals of Warsaw University of Life Sciences - SGGW. Land Reclamation 45, pp 183-192, 2013.
12. K. Pawluk, G. Wrzesiński, M. Lendo-Siwicka, "Strength and numerical analysis in the design of permeable reactive barriers", IOP Conference Series: Materials Science and Engineering 245, pp 1-8, 2017.
13. R.J. Jardine, C.O. Menkiti, "The undrained anisotropy of K_o consolidated sediments", Proc. of 12th European Conference on Soil Mechanics and Geotechnical Engineering, Amsterdam, 2, pp 1101-1108, 1999.
14. J.R.F. Arthur, B.K. Menzies, "Inherent anisotropy in a sand", Géotechnique 22, pp 115-128, 1972.
15. J.R.F. Arthur, K.S. Chua, T. Dunstan, C.J.I. del Roderiguez, "Principal stress rotation: a missing parameter", Journal of the Geotechnical Engineering Division 106, pp 419-433, 1980.
16. H. Ohta, A. Nishihara, "Anisotropy of undrained shear strength of clays under axi-symmetric loading conditions", Soils and Foundations 25, pp 73-86, 1985.
17. L. Bjerrum, A. Landva, "Direct simple-shear tests on a norvegian quick clay", Géotechnique 16, pp 1-20, 1966.
18. D.K. Wright, P.A. Gilbert, A.S. Saada, "Shear devices for determining dynamic soil properties", Proc. Specialty Conference on Earthquake Engineering and Soil Dynamics, ASCE, 2, pp 1056-1075, 1978.

19. W.H. Ward, S.G. Samuels, M.E. Butler, “Further studies of the properties of the London Clay”, Géotechnique 9, pp 33-58, 1959.
20. J.H. Atkinson, “Anisotropic elastic deformations in laboratory tests on undisturbed London Clay”, Géotechnique 25, pp 357-374, 1975.
21. T. Shogaki, N. Kumagai, “A slope stability analysis considering undrained strength anisotropy of natural clay deposits”, Soils and Foundations 48, pp 805-819, 2008.
22. K. Miura, S. Miura, S. Toki, “Deformation behavior of anisotropic dense sand under principal stress axes rotation”, Soils and Foundations 26, pp 36-52, 1986.
23. K. Ishihara, I. Towhata, “Sand response to cyclic rotation of principal stress directions as induced by wave loads”, Soils and Foundations 23, pp 11-26, 1983.
24. S. Yamashita, S. Toki, “Effects of fabric anisotropy of sand on cyclic undrained triaxial and torsional strengths”, Soils and Foundations 33, pp 92-104, 1993.
25. Y.P. Vaid, A. Eliadorani, S. Sivathayalan, R.M. Uthayakuma, “Laboratory characterization of stress-strain behavior of soils by stress and/or stress path loading”, Geotechnical Testing Journal 24, pp 200-208, 2001.
26. Z.X. Yang, X.S. Li, J. Yang, “Undrained anisotropy and rotational shear in granular soil”, Géotechnique 57, pp 371-384, 2007.
27. S.K. Chaudhary, J. Kuvano, Y. Hayano, “Measurement of quasi-elastic stiffness parameters of dense toyoura sand in hollow cylinder apparatus and triaxial apparatus with bender elements”, Geotechnical Testing Journal 27, pp 1-13, 2004.
28. A.S. Saada, F.C. Townsend, “State of the Art: Laboratory strength testing of soils”, ASTM STP 740, pp 7-77, 1981.
29. M. Jamiołkowski, C.C. Ladd, J.T. Germaine, R. Lancelotta, “New developments in field and laboratory testing of soils”, Proc. of 11th International Conference on Soil Mechanics and Foundation Engineering, San Francisco, 1, pp 57-153, 1985.
30. EN ISO 14688-1, “Geotechnical investigation and testing – identification and classification of soil – Part 1: Identification and description”, International Organization for Standardization, Geneva, Switzerland, 2002.
31. EN ISO 14688-2, “Geotechnical investigation and testing – identification and classification of soil – Part 2: Principles for a classification”, International Organization for Standardization, Geneva, Switzerland, 2004.
32. A.W. Bishop, “The strength of soils as engineering materials”, Géotechnique 16, pp 91–130, 1966.
33. G. Wrzesiński, Z. Lechowicz, “Testing of undrained shear strength in a hollow cylinder apparatus”, Studia Geotechnica et Mechanica 37, 69-73, 2015.
34. G. Wrzesiński, “Stability analysis of an embankment with influence of principal stress rotation on the shear strength of subsoil”, Ph.D. Thesis, Warsaw University of Life Sciences, Poland, 2016.
35. G. Wrzesiński, M. Sulewska, Z. Lechowicz, “Evaluation of the change in undrained shear strength in cohesive soils due to principal stress rotation using an artificial neural network”, Applied Sciences-Basel 8, pp 1-12, 2018.
36. G. Wrzesiński, K. Pawluk, M. Lendo-Siwicka, A. Miszkowska, “Undrained shear strength anisotropy of cohesive soils caused by the principal stress rotation”, IOP Conference Series: Materials Science and Engineering 471, pp 1-8, 2019.
37. F. Tavenas, “Some aspects of clay behavior and their consequences on modeling techniques”, Laboratory shear strength of soil. ASTM STP 740, pp 667-677, 1981.

LIST OF FIGURES AND TABLES:

ANIZOTROPIA PARAMETRÓW WYTRZYMAŁOŚCIOWYCH W GRUNTACH SPOWODOWANA OBROTEM KIERUNKÓW NAPRĘŻEŃ GŁÓWNYCH

Keywords: grunt, wytrzymałość na ścinanie bez odpływu, efektywna spójność, efektywny kąt tarcia wewnętrznego, obrót kierunków naprężeń głównych, badanie w cylindrycznym aparacie skrętnym, badanie w aparacie trójosiowym

STRESZCZENIE:

W artykule przedstawiono wpływ obrotu kierunków naprężeń głównych na wartości parametrów wytrzymałościowych gruntów spoistych: wytrzymałość na ścinanie bez odpływu τ_{fu}, efektywną spójność c', efektywny kąt tarcia wewnętrznego φ'. W tym celu przeprowadzono badania w aparacie trójosiowym i w cylindrycznym aparacie skrętnym na wybranych gruntach spoistych o nienaruszonej strukturze: sasiCl, saclSi, clSi, Cl o różnych wartościach parametrów fizycznych. Badano grunty o współczynniku prekonsolidacji *OCR* w zakresie od 1.1 do 5.7, wskaźniku plastyczności I_p w zakresie od 10.0% do 83.8% oraz wskaźniku konsystencji I_c w zakresie od 0.14 do 1.16. Parametry wytrzymałościowe gruntów określono przy kątach obrotu kierunków naprężeń głównych α równych 0° i 90° w badaniach w aparacie trójosiowym i kątach α równych 0°, 15°, 30°, 45°, 60°, 75°, 90° w badaniach w cylindrycznym aparacie skrętnym. Wyniki badań laboratoryjnych pozwoliły ocenić wpływ obrotu kierunków naprężeń głównych na parametry wytrzymałościowe gruntów spoistych niezbędnych przy wyznaczaniu nośności podłoża.

Badania przeprowadzone w aparacie trójosiowym i cylindrycznym aparacie skrętnym wykazały, że obrót kierunków naprężeń głównych powoduje anizotropię parametrów wytrzymałościowych: wytrzymałości na ścinanie bez odpływu τ_{fu}, efektywnej spójności c', efektywnego kąta tarcia wewnętrznego φ'. W gruntach normalnie skonsolidowanych ($OCR \approx 1$) wartość parametrów wytrzymałościowych jest zasadniczo najniższa przy kącie obrotu kierunków naprężeń głównych $\alpha = 45°$, natomiast w przypadku gruntów prekonsolidowanych ($OCR \geq 2$) wartość parametrów wytrzymałościowych maleje wraz ze wzrostem kąta obrotu kierunków naprężeń głównych α. Badania przeprowadzone w aparacie trójosiowym przy kątach α równych 0° i 90° oraz w cylindrycznym aparacie skrętnym przy tych samych wartościach kątów α pokazują, że dla wszystkich gruntów spoistych uzyskano mniejszą wartość parametrów wytrzymałościowych w badaniach w aparacie trójosiowym.

Zjawisko obrotu kierunków naprężeń głównych w podłożu w wyniku zmian obciążenia jest zjawiskiem powszechnym, jednak ze względu na trudność w określeniu jego wpływu na parametry wytrzymałościowe w badaniach laboratoryjnych jest powszechnie pomijane. Prowadzi to do tego, że w obliczeniach nośności podłoża stosuje się najczęściej tylko jedną wartość parametrów wytrzymałościowych, najczęściej określonych pod kątem $\alpha = 0°$. Przyjęcie wartości parametrów wytrzymałościowych określonych przy jednym kącie obrotu kierunków naprężeń głównych α dla całego podłoża najczęściej prowadzi do niedoszacowania lub przeszacowania rzeczywistej wartości nośności podłoża.

Received: 26.06.2020, Revised: 12.10.2020

.